

PS INSAR TECHNIQUE AND ITS APPLICATION IN BEIJING AREA

Bai Jun Veronique PRINET

National Laboratory of Pattern Recognition (NLPR)
Sino-French Laboratory in Information, Automation and Applied Mathematics (LIAMA)
Institute of Automation, Chinese Academy of Sciences - PoBox 2728 - Beijing 100080 – PR China
Fax : 86-10 62647458 tel : 86-10 82614462
jbai@nlpr.ia.ac.cn prinet@nlpr.ia.ac.cn

KEY WORDS: Permanent Scatters, SAR interferometry, Line of Sight velocity, Subsidence, Topographic deformation, Radar image, Urban area, Application

ABSTRACT:

PS InSAR (Permanent Scatters for Interferometric Synthetic Aperture Radar) was proposed at first by A.Ferretti in 2001(Ferretti, 2001). In this technique, stable natural reflectors or permanent scatters are detected and studied over long temporal series of interferometric SAR images, in order to detect and measure topographic changes. PS technique has already shown remarkable potentials and has proved to be a powerful tool for exploring slow movements of Earth surface. In this paper, we introduce a new approach for PS point selection, namely the “Amplitude Filter”. We propose some improvement of the elevation change velocity computational algorithmic. Application is carried out with a limited set of 13 ERS1 and ERS2 images from 1995 to 1999, covering Beijing city area in China, completed with a SRTM-3 data (Shuttle Radar Topography Mission) to serve as digital elevation model (DEM). Results and illustrations are shown on a sample area of about a 5x20 km .

I. INTRODUCTION

Permanent Scatters SAR Interferometry (PSInSAR) is a unique and new technique in the field of SAR Interferometry (InSAR) processing. Since it was introduced in 2001(Ferretti, 2001), it has proved to be a powerful tool to explore the subsidence of topography with high accuracy, i.e up to few millimeters(Ferretti, 2001;Ferretti, 2000). It has been in these recent years an active topic for both research and development applications.

In PS-InSAR technique, a large set of SAR images (generally more than 20) are used. Only stable pixels on a sparse grid, i.e. pixels that are coherent over long time intervals are selected and explored. These pixels are called Permanent Scatters (PSs). Once PSs are detected, a reference Digital Elevation Model (DEM) can be used to subtract the topography phase; then the line of sight (LOS) velocity and the atmospheric phase screen (APS) can be estimated. Additionally, further refinement of LOS velocity and APS can be carried out when necessary. Generally, the processing includes the following steps:

i. Interferogram Generation: Having $K+1$ SAR images, K interferograms are generated with full-resolution. The phase term caused by flat Earth is removed in this step.

ii. PS Identification: Applying some criteria on coherence or amplitude values, a set of pixels is selected as PSs. Further study can then be carried out in this sub-set of images pixels.

iii. Topography Phase Removal: Given a reference DEM and with the DEOS precise orbit data (Scharroo.R), the topography phase can be estimated and removed. In fact, this work can be carried out only in the subset of selected PSs. If the entire

image is processed, it is the differential interferogram formation step (Ferretti, 2001).

iv. LOS velocity and DEM Error Estimation: After step *iii*, the phase residue still contains the atmospheric term, phase caused by the DEM error, LOS motion term and noise. These terms can be computed via optimization. Usual approaches are iteration algorithm (Ferretti, 2001), or network integration method (Kamps , 2004).

The main goal of this paper is to apply PS technique in the area of Beijing, China, to measure the subsidence rate of the city in the recent years. The contributions of this paper are : *i*) to propose a new approach for PS point selection ; *ii*) to simplify the calculation of the PS model solution. Our original framework for PS detection is detailed in section II. A new concept named “Amplitude Filter” is introduced, adding more constraints on PS detection. In section III, topographic phase of the selected PSs is estimated and removed, according to the ellipsoid model. In section IV the LOS velocity is estimated. Based on an iterative algorithm proposed by A.Ferretti & al. (Ferretti, 2001), we propose some improvements to get more robust computation. In section V, experimental results are presented. Conclusions and future work are given in the final section.

II. SELECTION OF PERMANENT SCATTERS

The problem is how to detect stable point scatters from a set of images. Related works can be found in (Ferretti, 2001;Adam, 2003). Two different methods have been proposed: the coherence approach and the amplitude approach. In the coherence approach, pixels that exhibit high coherence values in all interferograms are selected as PS candidates. However,

when estimating coherence, a spatial correlation window must be used, leading to a spatial average effect. This is indeed an undesirable effect since we expect PS points to locate targets on the ground having a size close to or smaller than the pixel resolution.

Table 1:List of ERS1,2 SAR images

SAT(ERS1/2)	Orbit	Date	Normal Baseline (m)	Temporal Baseline (day)	Height Ambiguity (m)
ERS2	17607	19980902	0	0	-----
ERS2	03579	19951227	198.6	-980	44.3917
ERS2	06585	19960724	90.8	-770	97.0946
ERS2	07086	19960828	-882.4	-735	-9.9911
ERS2	12096	19970813	-80.9	-385	-108.9764
ERS2	12597	19970917	-786.5	-350	-11.2094
ERS1	32771	19971021	-499.7	-316	-17.6430
ERS2	16104	19980520	93.6	-105	94.19
ERS2	16605	19980624	153.7	-70	57.3597
ERS2	17106	19980729	-245.1	-35	-35.9698
ERS2	18108	19981007	379.8	35	23.2127
ERS2	21615	19990609	52.5	280	167.9274
ERS2	22617	19990818	1044.3	350	8.4422
ERS2	38649	20020911	205	1470	43.0058
ERS2	39150	20021016	-316	1505	-27.8993

Here we use the second approach, studying the amplitude values of each pixel in the images. A.Ferretti has proposed a measure of phase stability (Ferretti, 2001)

$$D_A = \frac{\sigma_A}{m_A} \tag{1}$$

In equation (1) m_A and σ_A are the mean and standard deviation of the amplitude values of a given pixel over all the set of images. A.Ferretti & al. has proved that when many SAR images are available, the amplitude dispersion D_A can be safely considered as the phase dispersion. In fact, equation (1) means simply that when the amplitude value of a pixel over all the images changes is almost constant, this pixel is stable and can be selected as a PS candidate.

From experimentation, we noticed that some pixels with low amplitude values, in lakes areas for example, also exhibit the stable amplitude value characteristic. That means, at these pixels, although the mean amplitude value is low, the standard deviations are lower, resulting in a low amplitude dispersion value and these pixels would be selected as PSs. But indeed these pixels, which also exhibits low coherence, should not be retained.

For this reason, we developed the concept of “Amplitude Filter”, adding an adaptive threshold to the processing of PSs detection. On one hand we use the amplitude dispersion as one estimator. On the other hand, we consider the amplitude values of the pixels. Only the pixels with the amplitude values larger than a certain threshold have the chance to be selected as PSs.

The problem is how to define an amplitude threshold. It is not suitable to define an absolute value since the amplitude value is affected by many factors –backscattering coefficient, noise, etc. However, we can define a relative value, i.e. relative to the spacing average of the whole area of interest. Let’s at first ignore the threshold for amplitude dispersion and consider the following strategy: For each pixel, calculate the average amplitude over all the available images. Thus we get an “average amplitude image”. Create an histogram of this “image” in an inversed sequence, with large values ahead and small values behind. Then we can declare that only a certain percentage of pixels ahead have the chance to be selected as PSs. The choice of the percentage of pixels selection determines the threshold for amplitude. The percentage value is obtained empirically. From our experimentation, 5 percent provides satisfying results.

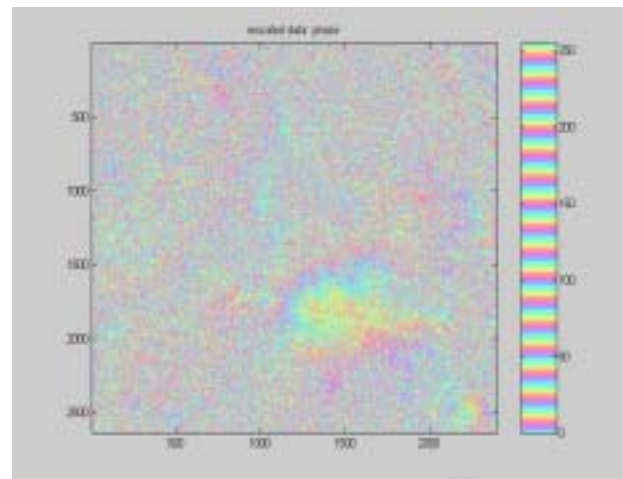
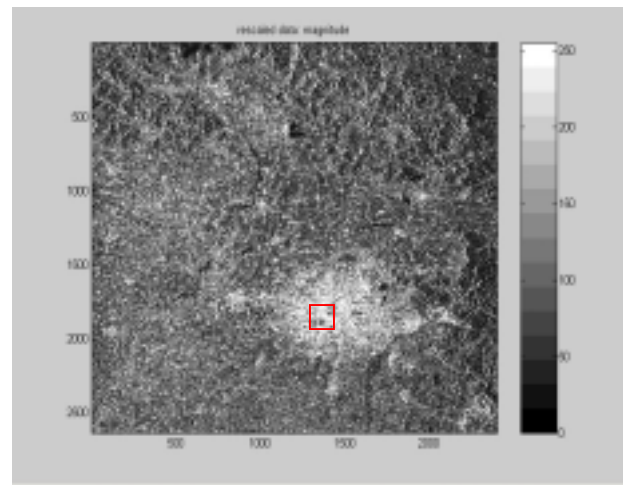


Figure 1:Up: Amplitude image on the area covering Beijing
Down: Associated interferogram from SAR-ERS images acquired at 98/09/02 and 99/06/09, after flattening.
Normal Baseline: 52.5m, Height Ambiguity:167.2 m

In summary, an “Amplitude Filter” of 0.5 means only 0.5 percent of pixels with highest amplitude values has the possibility to be selected as PSs. Other pixels are “filtered out”. Notice the amplitude value is the average over all the available images.

III. INTERFEROGRAM GENERATION AND TOPOGRAPHIC PHASE REMOVAL

Interferograms are created with pair-wise SAR complex data, using one unique reference image. This processing is performed using Doris software open source developed at Delft University (Kamps,1999;Kamps,2003). Illustration of an interferogram is given in figure 1.

Before the estimation of LOS velocity and APS, the topographic phase needs to be removed. This step is also called *differential interferograms generation*, or *zero baseline steering* (Ferretti, 2001). Existing DEM data is required to estimate the topographic phase.

The phase term caused by the topographic elevation q can be expressed as:

$$\phi_{qk}(x) = \frac{4\pi f}{c} B_n \frac{q(x)}{R_M(x) \sin \theta(x)} \quad (2)$$

In equation (2), f is the radar signal frequency, c light velocity. B_n is the normal baseline, which can be considered as a constant and is estimated when the interferogram is created. $R_M(x)$ is the master-sensor target distance. $\theta(x)$ is the local incidence angle. $q(x)$ is the elevation given from the DEM. Although some papers report that DEM can be generated by combining several tandem pairs of interferograms, we can more conveniently make use of the Shuttle Radar Topography Mission (SRTM) data. Since SRTM resolution is of about 90 meters in both azimuth and range, interpolation and resampling is needed to fit with the ERS images.

The two parameters that should be computed are $R_M(x)$ and $\theta(x)$. We can easily derive $R_M(x)$ from the range time of the pixel, calculated by the first range time and the range position of the pixel. With ellipsoid model and precise orbit data, we can also retrieve the incidence angle $\theta(x)$.

Figure 2 shows the geometry. \bar{X}_s and \bar{X} are respectively sensor vector and scatter vector, which can be acquired from precise orbit data and the scatter position. From geometry we can get the equation of incidence angle:

$$\theta = \arccos \frac{(\bar{X}_s - \bar{X}) \bullet \bar{X}}{\left| (\bar{X}_s - \bar{X}) \right| \left| \bar{X} \right|} \quad (3)$$

Once the topographic phase is computed, the orbital phase and topographic phase are both removed from the interferogram. The residue, or differential interferogram, can be considered as interferogram with zero baselines (Ferretti, 2001). The processing is indeed applied to each of the interferograms.

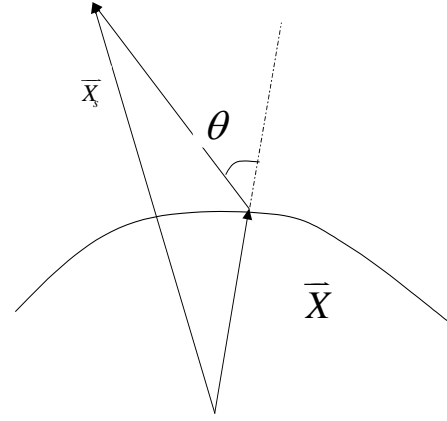


Figure 2: Geometry of the satellite-ellipsoid model

IV. SYSTEM SOLUTION AND LOS VELOCITY ESTIMATION

A.Ferretti&al has given a model for the components of the *zero-baseline steered* interferometric phases (Ferretti, 2001):

$$\Delta\phi = a1^T + p_\xi \xi^T + p_\eta \eta^T + B\Delta q^T + Tv^T + E \quad (4)$$

It is a matrix equations system of size $K \times H$, where K is the number of images and H is the number of PS points. The known parameters are:

- $\Delta\phi[K \times H]$: interferometric phase after the removing of the topographic phase and the flattened phase
- $\xi, \eta[H \times 1]$: azimuth and slant range position of the pixel
- $B, T[K \times 1]$: factors proportional to normal and temporal baselines respectively

The unknown parameters are:

- $a, p_\xi, p_\eta[K \times 1]$: constant and linear coefficients of phase residues along azimuth and range directions
- $\Delta q[H \times 1]$: elevation error of the DEM
- $v[H \times 1]$: LOS velocity
- E : remaining phase noise

An iterative algorithm was proposed in (A. Ferretti 2001) to solve the equation system (4). However, we can notice that equation (4) has not a unique solution, even within one period of 2π . Rather than $a, \Delta q, v$, let's show that $a - kT, \Delta q, v + k1$, can also be solution of the system $-k$ being any constant. Equation (4) can be re-written:

$$\begin{aligned} & (a - kT)1^T + p_\xi \xi^T + p_\eta \eta^T + B\Delta q^T + T(v + k1)^T + E \\ &= a1^T - kT1^T + p_\xi \xi^T + p_\eta \eta^T + B\Delta q^T + Tv^T + kT1^T + E \\ &= a1^T + p_\xi \xi^T + p_\eta \eta^T + B\Delta q^T + Tv^T + E \\ &= \Delta\phi \end{aligned} \quad (5)$$

From equation (5) we can see both sets of parameters are the solutions of the system.

In order to solve (4), we thus propose an original strategy. First we simplify the equation. Then additional conditions are added, trying to get the unique solution..

We can write equation (4) in its matrix form:

$$\begin{aligned}
 & \begin{bmatrix} \Delta\Phi_{11} & \Delta\Phi_{12} & \dots & \Delta\Phi_{1H} \\ \Delta\Phi_{21} & \Delta\Phi_{22} & \dots & \Delta\Phi_{2H} \\ \dots & \dots & \dots & \dots \\ \Delta\Phi_{K1} & \Delta\Phi_{K2} & \dots & \Delta\Phi_{KH} \end{bmatrix} = \begin{bmatrix} a_1 & a_1 & \dots & a_1 \\ a_2 & a_2 & \dots & a_2 \\ \dots & \dots & \dots & \dots \\ a_K & a_K & \dots & a_K \end{bmatrix} \\
 & + \begin{bmatrix} p_{\xi_1}\xi_1 & p_{\xi_1}\xi_2 & \dots & p_{\xi_1}\xi_H \\ p_{\xi_2}\xi_1 & p_{\xi_2}\xi_2 & \dots & p_{\xi_2}\xi_H \\ \dots & \dots & \dots & \dots \\ p_{\xi_K}\xi_1 & p_{\xi_K}\xi_2 & \dots & p_{\xi_K}\xi_H \end{bmatrix} + \begin{bmatrix} p_{\eta_1}\eta_1 & p_{\eta_1}\eta_2 & \dots & p_{\eta_1}\eta_H \\ p_{\eta_2}\eta_1 & p_{\eta_2}\eta_2 & \dots & p_{\eta_2}\eta_H \\ \dots & \dots & \dots & \dots \\ p_{\eta_K}\eta_1 & p_{\eta_K}\eta_2 & \dots & p_{\eta_K}\eta_H \end{bmatrix} \\
 & + \begin{bmatrix} B_1\Delta q_1 & B_1\Delta q_2 & \dots & B_1\Delta q_H \\ B_2\Delta q_1 & B_2\Delta q_2 & \dots & B_2\Delta q_H \\ \dots & \dots & \dots & \dots \\ B_K\Delta q_1 & B_K\Delta q_2 & \dots & B_K\Delta q_H \end{bmatrix} + \begin{bmatrix} T_1v_1 & T_1v_2 & \dots & T_1v_H \\ T_2v_1 & T_2v_2 & \dots & T_2v_H \\ \dots & \dots & \dots & \dots \\ T_Kv_1 & T_Kv_2 & \dots & T_Kv_H \end{bmatrix} \\
 & + \begin{bmatrix} E_{11} & E_{12} & \dots & E_{1H} \\ E_{21} & E_{22} & \dots & E_{2H} \\ \dots & \dots & \dots & \dots \\ E_{K1} & E_{K2} & \dots & E_{KH} \end{bmatrix} \tag{6}
 \end{aligned}$$

By averaging all columns of (6), we have:

$$\begin{aligned}
 & \begin{bmatrix} \overline{\Delta\Phi_1} \\ \overline{\Delta\Phi_2} \\ \dots \\ \overline{\Delta\Phi_K} \end{bmatrix} = \begin{bmatrix} a_1 \\ a_2 \\ \dots \\ a_K \end{bmatrix} + \begin{bmatrix} p_{\xi_1} \\ p_{\xi_2} \\ \dots \\ p_{\xi_K} \end{bmatrix} \overline{\xi} + \begin{bmatrix} p_{\eta_1} \\ p_{\eta_2} \\ \dots \\ p_{\eta_K} \end{bmatrix} \overline{\eta} \\
 & + \begin{bmatrix} B_1 \\ B_2 \\ \dots \\ B_K \end{bmatrix} \overline{\Delta q} + \begin{bmatrix} T_1 \\ T_2 \\ \dots \\ T_K \end{bmatrix} \overline{v} + \begin{bmatrix} \overline{E_1} \\ \overline{E_2} \\ \dots \\ \overline{E_K} \end{bmatrix} \tag{7}
 \end{aligned}$$

By subtracting (7) from (6) in each column, we have:

$$\begin{aligned}
 & \begin{bmatrix} \widehat{\Delta\Phi_{11}} & \widehat{\Delta\Phi_{12}} & \dots & \widehat{\Delta\Phi_{1H}} \\ \widehat{\Delta\Phi_{21}} & \widehat{\Delta\Phi_{22}} & \dots & \widehat{\Delta\Phi_{2H}} \\ \dots & \dots & \dots & \dots \\ \widehat{\Delta\Phi_{K1}} & \widehat{\Delta\Phi_{K2}} & \dots & \widehat{\Delta\Phi_{KH}} \end{bmatrix} = \begin{bmatrix} \overline{\Delta\Phi_{11}} - \overline{\Delta\Phi_{11}} & \overline{\Delta\Phi_{12}} - \overline{\Delta\Phi_{12}} & \dots & \overline{\Delta\Phi_{1H}} - \overline{\Delta\Phi_{1H}} \\ \overline{\Delta\Phi_{21}} - \overline{\Delta\Phi_{21}} & \overline{\Delta\Phi_{22}} - \overline{\Delta\Phi_{22}} & \dots & \overline{\Delta\Phi_{2H}} - \overline{\Delta\Phi_{2H}} \\ \dots & \dots & \dots & \dots \\ \overline{\Delta\Phi_{K1}} - \overline{\Delta\Phi_{K1}} & \overline{\Delta\Phi_{K2}} - \overline{\Delta\Phi_{K2}} & \dots & \overline{\Delta\Phi_{KH}} - \overline{\Delta\Phi_{KH}} \end{bmatrix} \\
 & + \begin{bmatrix} p_{\xi_1}(\xi_1 - \overline{\xi}) & p_{\xi_1}(\xi_2 - \overline{\xi}) & \dots & p_{\xi_1}(\xi_H - \overline{\xi}) \\ p_{\xi_2}(\xi_1 - \overline{\xi}) & p_{\xi_2}(\xi_2 - \overline{\xi}) & \dots & p_{\xi_2}(\xi_H - \overline{\xi}) \\ \dots & \dots & \dots & \dots \\ p_{\xi_K}(\xi_1 - \overline{\xi}) & p_{\xi_K}(\xi_2 - \overline{\xi}) & \dots & p_{\xi_K}(\xi_H - \overline{\xi}) \end{bmatrix} + \begin{bmatrix} p_{\eta_1}(\eta_1 - \overline{\eta}) & p_{\eta_1}(\eta_2 - \overline{\eta}) & \dots & p_{\eta_1}(\eta_H - \overline{\eta}) \\ p_{\eta_2}(\eta_1 - \overline{\eta}) & p_{\eta_2}(\eta_2 - \overline{\eta}) & \dots & p_{\eta_2}(\eta_H - \overline{\eta}) \\ \dots & \dots & \dots & \dots \\ p_{\eta_K}(\eta_1 - \overline{\eta}) & p_{\eta_K}(\eta_2 - \overline{\eta}) & \dots & p_{\eta_K}(\eta_H - \overline{\eta}) \end{bmatrix} \\
 & + \begin{bmatrix} B_1(\Delta q_1 - \overline{\Delta q}) & B_1(\Delta q_2 - \overline{\Delta q}) & \dots & B_1(\Delta q_H - \overline{\Delta q}) \\ B_2(\Delta q_1 - \overline{\Delta q}) & B_2(\Delta q_2 - \overline{\Delta q}) & \dots & B_2(\Delta q_H - \overline{\Delta q}) \\ \dots & \dots & \dots & \dots \\ B_K(\Delta q_1 - \overline{\Delta q}) & B_K(\Delta q_2 - \overline{\Delta q}) & \dots & B_K(\Delta q_H - \overline{\Delta q}) \end{bmatrix} \\
 & + \begin{bmatrix} T_1(v_1 - \overline{v}) & T_1(v_2 - \overline{v}) & \dots & T_1(v_H - \overline{v}) \\ T_2(v_1 - \overline{v}) & T_2(v_2 - \overline{v}) & \dots & T_2(v_H - \overline{v}) \\ \dots & \dots & \dots & \dots \\ T_K(v_1 - \overline{v}) & T_K(v_2 - \overline{v}) & \dots & T_K(v_H - \overline{v}) \end{bmatrix} + \begin{bmatrix} E_{11} - \overline{E_1} & E_{12} - \overline{E_2} & \dots & E_{1H} - \overline{E_H} \\ E_{21} - \overline{E_2} & E_{22} - \overline{E_2} & \dots & E_{2H} - \overline{E_2} \\ \dots & \dots & \dots & \dots \\ E_{K1} - \overline{E_H} & E_{K2} - \overline{E_H} & \dots & E_{KH} - \overline{E_H} \end{bmatrix} \tag{8}
 \end{aligned}$$

Or, in a simplified form, equation (8) can be written as:

$$\begin{aligned}
 \widehat{\Delta\phi} &= p_{\xi} \widehat{\xi} + p_{\eta} \widehat{\eta} + B \widehat{\Delta q} + T \widehat{v} + E' \tag{8} \\
 \text{with } \widehat{\xi} &= \xi - \overline{\xi}, \widehat{\eta} = \eta - \overline{\eta}, \widehat{\Delta q} = \Delta q - \overline{\Delta q}, \widehat{v} = v - \overline{v}.
 \end{aligned}$$

Comparing equation (8) with equation (4), we can see that the constant term disappears. We can yet solve the equation system, with one less unknown. We can then get an estimation of $\widehat{\Delta q}$ and \widehat{v} .

The following shows how to derive the original parameters a , Δq , v . To reach our goal, additional conditions must be assumed:

i. *The expectation of DEM error*

We can get this from the handbook of DEM product. In general, we can suppose that:

$$\begin{aligned}
 E\{\Delta q_h\} &= 0 \tag{9}
 \end{aligned}$$

Then we have:

$$\Delta q_h = \widehat{\Delta q}_h + \overline{\Delta q} \triangleq \widehat{\Delta q}_h + E\{\Delta q_h\} \tag{10}$$

ii. *The statistic characteristic of APS*

Commonly we can consider that the APS at different time is random. Notice at the same time a is the constant term of APS. Then we can have:

$$E\{a_m a_n\} = E\{a_m\} E\{a_n\} \tag{11}$$

In (12), $E\{a_m a_n\}$ and $E\{a_k\}$ can be estimated as:

$$E\{a_m a_n\} = \frac{2}{(K-1)(K-2)} \sum_m \sum_{n \neq m} a_m a_n \tag{12}$$

$$E\{a_n\} = \frac{1}{K} \sum_n a_n \tag{13}$$

From equation (5) we can conclude that the right solution of equation (4) can be expressed as:

$$\begin{aligned}
 a &= -kT \\
 v &= \widehat{v} + k1 \tag{14}
 \end{aligned}$$

According to (11)-(15) we can finally get the solution of a , Δq , v .

V. EXPERIMENTAL RESULTS

(8) Our application site is Beijing area, China, centered at longitude of 116.35 E and latitude of 39.9 N, for which we wish to estimate the subsidence rate. The image set includes 13 ERS1,2, from 1995 to 1999. For the restriction of APS model, we select a small area of $5 \times 20 \text{ km}^2$ (illustrated by the small square in the amplitude image of figure 1). Figure 1 gives the

list of the images and their basic characteristics. Using Doris software (Kamps,1999;Kamps,2003), 12 interferograms are created, the flat phase is removed. In the step of PS detection, experiment and comparison are done without “Amplitude Filter”, and with an “Amplitude Filter” of 1,2 and 5. Finally we use the “Amplitude Filter” of 5 and 467 PS points are selected. Figure 3 shows the increasing of PSs with the change of “Amplitude Filter”. PSs distributions for selected without “Amplitude Filter” and with “Amplitude Filter” of 1 and 5 are illustrated in Figure 4.

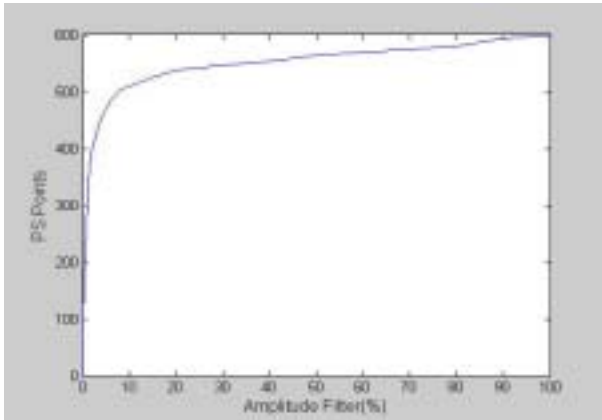
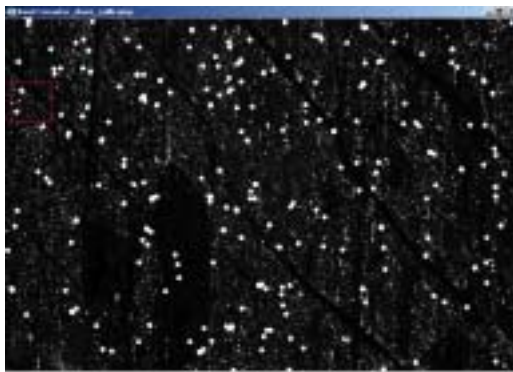
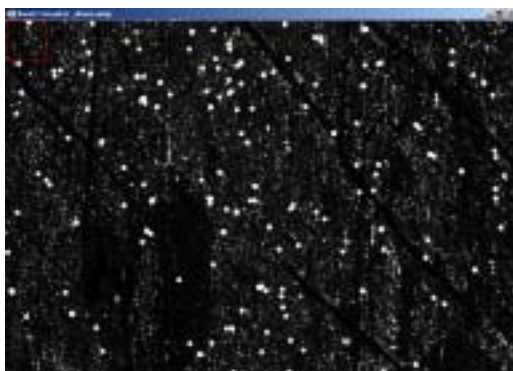


Figure 3. The number of PS points with the change of Amplitude Filter



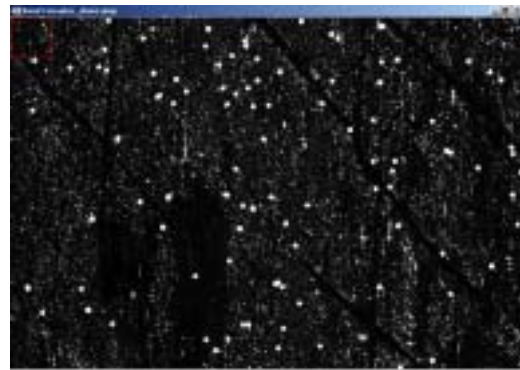
4.a. No Amplitude Filter (600 PSs)



4.b. Amplitude Filter 5 (467 PSs)

By using SRTM3 data, the topographic phase is estimated and removed. With our modified algorithm and after a few iterations the LOS velocity is estimated.

Figure 5 shows the LOS velocity of PS points overlapped on one of the SAR amplitude image. The bright rings outside show the positions of PSs, and the gray level inside the ring expresses the value of LOS velocity, ranging from about -8 mm/year to 6 mm/year.



4.c. Amplitude Filter 1 (305 PSs)

Figure 4. Comparisons of PS distribution for different Amplitude Filter threshold values

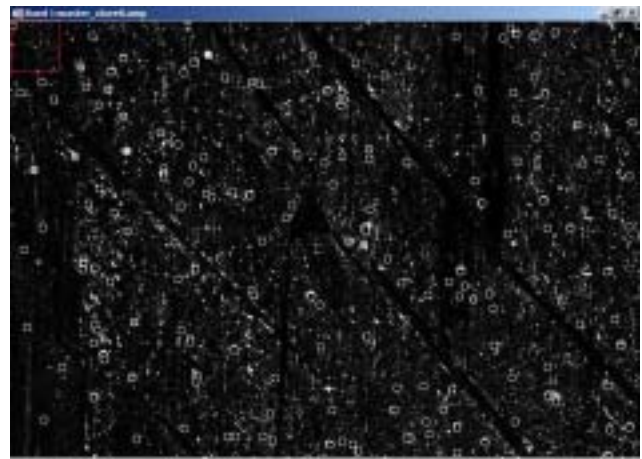


Figure 5. LOS velocity computed at each PS point superimposed on one SAR amplitude image

VI. CONCLUSIONS AND FURTHER WORK

PS technique has proved to be a unique tool for the analysis of subsidence. We have proposed a new scheme for PS point selection, based on an adaptative thresholding approach, in order to solve the problem of site-dependant threshold evaluation. A new algorithmic of the linear equation system have been developed in an attempt to find the unique solution.

However, our test case and experiments over Beijing city show certain limitations. In particular, it has been done with a limited number of images: this is in contradiction with most literature which advice to use a set of more 20 images; it therefore forgives us from any direct interpretation of the computed subsidence rate values. Other limitation concerns the model itself : the terrain motion may not be linear, although it is a basic assumption of equation (4). We may need to work out on more sophisticated model..

In order to increase the data set, we will need to make use of ENVISAT images. We are presently working on cross-interferometry and PS points from cross-interferograms,.

Acknowledgement

This work is supported by the Chinese Ministry of Sciences 863 program. Images have been provided by ESA, in the context of an AO3 project.

References

- Adam.N, Kamps.B, Eineder.M 2003 The Development of a Scientific Permanent Scatterer System *ISPRS Journal of Photogrammetry and Remote Sensing*
- Adam.N, Kamps.B, Eineder.M 2004 Development of a Scientific Permanent Scatterer System: Modifications for Mixed ERS/ENVISAT Time Series *ERS-ENVISAT Symposium*
- Ferretti.A, Prati.,C, Rocca.F 1999 Multibaseline InSAR DEM reconstruction: the wavelet approach *IEEE Transactions on Geoscience and Remote Sensing*, Vol. 37, No. 2, March 1999
- Ferretti.A, Prati.C, Rocca.F 2000 Nonlinear Subsidence Rate Estimation Using Permanent Scatterers in Differential SAR Interferometry *IEEE Transactions on Geoscience and Remote Sensing*, Vol.38, No.5, Sep.2000
- Ferretti A., Prati C., Rocca F. 2001 Permanent Scatterers in SAR Interferometry *IEEE Transactions on Geoscience and Remote Sensing*, Vol.39, No.1, January 2001
- Kamps.B Stefania.U. 1999 Doris: The Delft object-oriented Radar Interferometric software. *ITC 2nd ORS symposium*, August 1999
- Kamps.B, Hanssen.R, Perski.Z. 2003 Radar Interferometry with Public Domain Tools. *FRINGE 2003*, December 1-5, Frascati, Italy
- Kamps.B, Adam.N 2004 Deformation Parameter inversion using Permanent Scatterers in Interferogram *Time SeriesEUSAR'04*, Ulm, Gemrany, pages 341-344
- Scharroo.R, Doornbos.E ERS Precise Orbit Determination: Orbits
<http://www.deos.tudelft.nl/ers/precorbs/orbits/>